

Self-energy correction to the $E1$ transition amplitudes in hydrogen-like ions

M. G. Kozlov^{1,2}, M. Y. Kaygorodov¹, Yu. A. Demidov^{1,2}, and V. A. Yerokhin³

¹ Petersburg Nuclear Physics Institute NRC “Kurchatov Institute”, Gatchina 188300, Russia

² St. Petersburg Electrotechnical University “LETI”, St. Petersburg 197376, Russia

³ Peter the Great St. Petersburg Polytechnic University, St. Petersburg 195251, Russia

We present calculations of the self-energy correction to the $E1$ transition amplitudes in hydrogen-like ions, performed to all orders in the nuclear binding strength parameter. Our results for the $1s-2p_{1/2}$ transition for the hydrogen isoelectronic sequence show that the perturbed-orbital part of the self-energy correction provides the dominant contribution, accounting for approximately 99% of the total correction for this transition. Detailed calculations were performed for $ns-n'p$ and $np-n'd$ transitions in H-like cesium. We conclude that the perturbed-orbital part remains dominant also for other $ns-n'p$ transitions, whereas for the $np-n'd$ matrix elements this dominance no longer holds. Consequently, the self-energy corrections for the $np-n'd$ one-electron matrix elements cannot be well reproduced by means of effective QED operators constructed for energy levels.

I. INTRODUCTION

The rapid progress of experimental techniques in atomic spectroscopy, combined with improved computational methods developed for many-electron systems, requires the inclusion quantum electrodynamics (QED) corrections, not only for energy levels but also for other properties of many-electron atoms. In particular, recent large-scale many-body calculations of $E1$ transition amplitudes for neon-like iron and nickel have reached such high computational precision that the inclusion of QED effects has become mandatory [1–3].

An accurate knowledge of the transition amplitudes in many-electron atoms is necessary for the atomic tests of the standard model and in the search for the new physics beyond standard model [4]. For example, it is important to include QED corrections to the parity non-conserving transition amplitude in Cs [5] when comparing theory with the experiment [6]. QED corrections to the dynamic polarizability may affect magic frequencies for the clock transitions.

So far ab initio QED calculations have been conducted primarily for atoms and ions with one or several electrons; extending such methods to many-electron systems looks unfeasible at present. It is possible to perform ab initio QED calculations in many-electron systems within one-electron approximation [7, 8], but the omitted electron-correlation effects can be very significant in this case.

Most of recent calculations of $E1$ transition amplitudes of many-electron atoms performed so far [2, 3, 9–12] accounted for QED effects by using approximate methods based on different variants of effective QED potentials. The most successful of these is the model operator introduced by Shabaev and coworkers in Ref. [13] and implemented as QEDMOD package [14, 15]. It is important that the QEDMOD operator, as well as all other effective QED potentials, is designed to approximately reproduce QED effects for energy levels only. As a result, using these operators for calculations of transition amplitudes yields incomplete results, as they account only for part of the effect while neglecting other contributions, such as vertex and reducible corrections.

To justify the omission vertex and reducible corrections, the studies [2, 3, 9, 10] cited the work of Sapirstein and Cheng [16], who performed ab initio calculations of $E1$ transition

amplitudes for alkali atoms within the one-electron screening-potential approximation and found these corrections to be relatively small. However, Sapirstein and Cheng’s study focused solely on the $ns-np_{1/2}$ transition and was performed for a few alkali-like atoms, leaving the broader applicability of this statement uncertain. In our previous work [17], we performed one-electron ab initio calculations for neon-like iron and similarly concluded that the vertex and reducible corrections are small enough to be neglected at the current level of precision. Nonetheless, the general validity of this conclusion remains unclear.

The QED correction to the $E1$ transition amplitude consists of the electron self-energy and the vacuum-polarization parts. The vacuum-polarization part is relatively simple and can be easily accounted for, e.g., by means of vacuum-polarization potentials included into the QEDMOD package. By contrast, the self-energy part is much more complicated as it cannot be successfully approximated by a local potential.

In this work, we conduct a detailed study of the self-energy correction to the $E1$ transition amplitudes in hydrogen-like ions, with a particular focus on hydrogen-like cesium. The total self-energy contribution is divided into two parts: the perturbed-orbital (po) part, which can be approximately represented by effective QED potentials, and the vertex+reducible (vr) part, which is omitted by them. We analyze the relative effect of the vr part on the total self-energy correction for various transitions. Additionally, we examine the accuracy of the QEDMOD potential in approximating ab initio self-energy results. This information is required for assessing potential errors when using the QEDMOD operator in many-electron calculations of the $E1$ transition amplitude.

In this paper we use the relativistic units $m = \hbar = c = 1$ and the Heaviside charge units $\alpha = e^2/(4\pi)$.

II. BASIC FORMULAS

The $E1$ transition amplitude in the length gauge between the one-electron states a and b is given by the expectation value of the electric dipole operator,

$$z_{ab} = \langle a | r_z | b \rangle, \quad (1)$$

where r_z is the z component of the position vector \mathbf{r} .

The self-energy correction to the matrix element z_{ab} is represented as a sum of the perturbed-orbital (po) and the vertex+reducible (vr) parts,

$$\delta z_{se} = z_{po} + z_{vr}. \quad (2)$$

General formulas for these corrections were reported in the literature [16] (see also Ref. [18]). The perturbed-orbital part is given by

$$z_{po} = \sum_{n \neq a} \langle a | \Sigma_R(\varepsilon_a) | n \rangle \frac{z_{nb}}{\varepsilon_a - \varepsilon_n} + \sum_{n \neq b} \frac{z_{an}}{\varepsilon_b - \varepsilon_n} \langle n | \Sigma_R(\varepsilon_b) | b \rangle, \quad (3)$$

where $\Sigma_R(\varepsilon)$ is the renormalized one-loop self-energy operator, $\Sigma_R(\varepsilon) = \Sigma(\varepsilon) - \gamma^0 \delta m$, and δm is the one-loop mass counterterm. The one-loop self-energy operator is defined by its matrix elements with one-electron wave functions as [19]

$$\langle a | \Sigma(\varepsilon) | b \rangle = \frac{i}{2\pi} \int_{-\infty}^{\infty} d\omega \sum_n \frac{\langle an | I(\omega) | nb \rangle}{\varepsilon - \omega - u\varepsilon_n}, \quad (4)$$

where $u = 1 - i0$, the summation is performed over the complete spectrum of the Dirac equation and $I(\omega)$ describes the exchange by a virtual photon. In the Feynman gauge, $I(\omega)$ is given by

$$I(\omega, \mathbf{r}_1, \mathbf{r}_2) = \alpha (1 - \boldsymbol{\alpha}_1 \cdot \boldsymbol{\alpha}_2) \frac{e^{i\sqrt{\omega^2 + i0} r_{12}}}{r_{12}}, \quad (5)$$

with $r_{12} = |\mathbf{r}_1 - \mathbf{r}_2|$.

The vertex+reducible contribution is given by

$$z_{vr} = \frac{i}{2\pi} \int_{-\infty}^{\infty} d\omega \times \left[\sum_{n_1 n_2} \frac{z_{n_1 n_2} \langle an_2 | I(\omega) | n_1 b \rangle}{(\varepsilon_a - \omega - u\varepsilon_{n_1})(\varepsilon_b - \omega - u\varepsilon_{n_2})} - \frac{z_{ab}}{2} \sum_n \frac{\langle an | I(\omega) | na \rangle}{(\varepsilon_a - \omega - u\varepsilon_n)^2} - \frac{z_{ab}}{2} \sum_n \frac{\langle bn | I(\omega) | nb \rangle}{(\varepsilon_b - \omega - u\varepsilon_n)^2} \right]. \quad (6)$$

A. Angular integration

Using the standard Racah algebra, we evaluate the leading-order $E1$ transition matrix element z_{ab} as

$$z_{ab} = \frac{(-1)^{j_b - \mu_b}}{\sqrt{3}} C_{j_a, \mu_a, j_b, -\mu_b}^{1,0} C_1(\kappa_a, \kappa_b) r_{ab} \equiv \mathcal{P}_{ab} r_{ab}, \quad (7)$$

where $C_{j_1, m_1, j_2, m_2}^{j, m}$ is the Clebsch-Gordan coefficient, $C_L(\kappa_1, \kappa_2)$ is the reduced matrix element of the normalized

spherical harmonics, see, e.g., Eq. (A10) of Ref. [20], and the radial integral is defined as

$$r_{ab} = \int_0^\infty dr r^3 [g_a(r) g_b(r) + f_a(r) f_b(r)], \quad (8)$$

where $g(r)$ and $f(r)$ are the upper and lower radial components of the Dirac wave functions. The angular factor \mathcal{P}_{ab} introduced in Eq. (7) is the common prefactor for all corrections to z_{ab} .

For the evaluation of the vertex correction, we need to perform the angular integration in the following expression

$$X_{n_1 n_2} = \sum_{\mu_1 \mu_2} z_{n_1 n_2} \langle an_2 | I(\omega) | n_1 b \rangle, \quad (9)$$

where μ_1 and μ_2 are the momentum projections of the states n_1 and n_2 , respectively. We make use of the standard partial-wave decomposition of the matrix element with $I(\omega)$

$$\langle an_2 | I(\omega) | n_1 b \rangle = \alpha \sum_L J_L(an_2 n_1 b) R_L(\omega, an_2 n_1 b), \quad (10)$$

where J_L contains all the dependence on the angular momenta projections and given by Eq. (39) of Ref. [20] and R_L are the standard two-body radial integrals defined in Appendix A of Ref. [20]. After performing summations over the momentum projections with help of formulas from [21], we obtain

$$X_{n_1 n_2} = \alpha \mathcal{P}_{ab} \sum_L r_{n_1 n_2} R_L(\omega, an_2 n_1 b) \times \frac{C_1(\kappa_1, \kappa_2)}{C_1(\kappa_a, \kappa_b)} (-1)^{j_1 - j_2} \left\{ \begin{matrix} j_2 & j_1 & 1 \\ j_a & j_b & L \end{matrix} \right\}. \quad (11)$$

B. Momentum-space reduction

In order to perform renormalization in the vertex+reducible term, we need to separate out the contribution of the free electron propagators and evaluate them in momentum space, with a covariant regularization of ultraviolet divergences. The divergent terms can be shown to cancel between the vertex and reducible parts, whereas the remaining finite contribution needs to be calculated in momentum space. So, we represent Eq. (6) as a sum the free part that contains the contribution of free electron propagators and the many-potential part which is the remainder,

$$z_{vr} = z_{vr}^{(0)} + z_{vr}^{(1+)}. \quad (12)$$

The general calculation procedure is similar to that developed in the previous studies, see, e.g., Ref. [22]. New features appear only in calculations of the free vertex part, which contains the vertex operator with the electric dipole operator in the momentum space. We therefore will describe this part of our calculation in some detail.

The Fourier transform of the electric dipole operator is given by the gradient of the Dirac δ function,

$$\mathbf{r}_z \xrightarrow{\text{Fourier}} i(2\pi)^3 \nabla_z \delta^3(\mathbf{q}), \quad (13)$$

where $\mathbf{q} = \mathbf{p} - \mathbf{p}'$ is the exchanged momentum. It is rather cumbersome to perform calculations with the above momentum-space expression for the electric dipole operator, because we need to perform the integration by parts analytically before carrying out the integration over the momentum in the vertex operator. For this reason, we choose to follow Ref. [23] and introduce a finite regularization parameter ρ , which makes the Fourier transform to be a continuous function,

$$\mathbf{r}_z e^{-(\rho r/2)^2} \xrightarrow{\text{Fourier}} -i \mathbf{q}_z \frac{16\pi^{3/2}}{\rho^5} e^{-q^2/\rho^2}. \quad (14)$$

We found that if we perform numerical calculation with a sufficiently small regularization parameter (typically, $\rho \approx 10^{-6}$), the error introduced by the regulator is completely negligible at the level of our interest. Moreover, only a small momenta region $|p - p'| \sim \rho$ contributes to the total integrals, so that numerical integrations are relatively simple in this case.

We thus write the free part of the vertex contribution as

$$z_{\text{ver}}^{(0)} = -i \frac{16\pi^{3/2}}{\rho^5} \int \frac{d^3\mathbf{p}}{(2\pi)^3} \int \frac{d^3\mathbf{p}'}{(2\pi)^3} e^{-q^2/\rho^2} \times \bar{\psi}_a(\mathbf{p}) \Gamma_R^0(\varepsilon_a, \mathbf{p}; \varepsilon_b, \mathbf{p}') (\mathbf{p}_z - \mathbf{p}'_z) \psi_b(\mathbf{p}'), \quad (15)$$

where $\bar{\psi}_a(\mathbf{p}) = \psi_a^\dagger(\mathbf{p})\gamma^0$ and Γ_R^0 is the time component of the renormalized free-electron vertex operator, see Appendix B of Ref. [24] for definition and explicit representation. We now use the following representation for the vertex operator sandwiched between two Dirac functions,

$$\begin{aligned} \bar{\psi}_a(\mathbf{p}) \Gamma_R^0(\varepsilon_a, \mathbf{p}; \varepsilon_b, \mathbf{p}') \psi_b(\mathbf{p}') &= \frac{\alpha}{4\pi} i^{l_a - l_b} \\ &\times \left[\mathcal{F}_1^{ab}(p, p', \xi) \chi_{\kappa_a \mu_a}^\dagger(\hat{\mathbf{p}}) \chi_{\kappa_b \mu_b}(\hat{\mathbf{p}}') \right. \\ &\left. + \mathcal{F}_2^{ab}(p, p', \xi) \chi_{-\kappa_a \mu_a}^\dagger(\hat{\mathbf{p}}) \chi_{-\kappa_b \mu_b}(\hat{\mathbf{p}}') \right], \quad (16) \end{aligned}$$

with explicit formulas for \mathcal{F}_1 and \mathcal{F}_2 given by Eqs. (A5) and (A6) of Ref. [22] and $p = |\mathbf{p}|$, $\hat{\mathbf{p}} = \mathbf{p}/p$, and $\xi = \hat{\mathbf{p}} \cdot \hat{\mathbf{p}}'$. Performing angular integrations, we obtain

$$\begin{aligned} z_{\text{ver}}^{(0)} &= \mathcal{P}_{ab} \frac{\alpha}{8\pi^{9/2}\rho^5} i^{l_a - l_b + 1} \\ &\times \int_0^\infty dp \int_0^\infty dp' \int_{-1}^1 d\xi (pp')^2 e^{-q^2/\rho^2} \\ &\times \left\{ \mathcal{F}_1^{ab}(p, p', \xi) \left[p' P_{l_a}(\xi) - p P_{l_b}(\xi) \right] \right. \\ &\left. + \mathcal{F}_2^{ab}(p, p', \xi) \left[p' P_{l_a}(\xi) - p P_{l_b}(\xi) \right] \right\}, \quad (17) \end{aligned}$$

where $l_a = |\kappa_a + 1/2| - 1/2$, $\bar{l}_a = |\kappa_a - 1/2| - 1/2$ and $P_l(\xi)$ is the Legendre polynomial. We note that $i^{l_a - l_b + 1}$ is real since $l_a - l_b + 1$ should be even, according to angular selection rules.

The remaining integrals in Eq. (17) were performed numer-

ically, after the change of variables according to

$$\begin{aligned} &\int_0^\infty dp \int_0^\infty dp' \int_{-1}^1 d\xi (pp')^2 F(p, p', \xi) \\ &= \int_0^\infty dx \int_0^x dy \int_y^x dq \frac{pp'q}{2} \left[F(p, p', \xi) + F(p', p, \xi) \right], \quad (18) \end{aligned}$$

where $p = (x + y)/2$, $p' = (x - y)/2$, $q^2 = p^2 + p'^2 - 2pp'\xi$.

C. Frequency dependent correction

In our calculations so far we used the low-frequency limit of the $E1$ -transition operator in the length gauge $D \propto r_z$, whose matrix elements reduce to the radial amplitude r_{ab} given by Eq. (8). The complete relativistic $E1$ -transition operator contains in addition the frequency-dependent part [25, 26], which is of order $O(2\pi r/\lambda)$ where λ is the transition wave length. The frequency-dependent contribution is very small for neutral and slightly ionized atoms, but become significant for heavy highly ionized ions [27]. In order to assess the uncertainty due to use of the low-frequency limit of the transition operator, we now discuss the frequency-dependent correction to the radial amplitude r_{ab} .

The radial amplitudes of the relativistic $E1$ transition operator in the length gauge were presented in Refs. [25, 26] for the case of photon absorption:

$$\begin{aligned} d_{ab} &= \frac{3}{k} \int_0^\infty r^2 dr \left\{ j_1(kr) \left[g_a(r)g_b(r) + f_a(r)f_b(r) \right] \right. \\ &\quad \left. + j_2(kr) \left[\frac{\kappa_a - \kappa_b + 2}{2} g_a(r)f_b(r) \right. \right. \\ &\quad \left. \left. + \frac{\kappa_a - \kappa_b - 2}{2} f_a(r)g_b(r) \right] \right\}, \quad (19) \end{aligned}$$

where $j_n(x) = \sqrt{\frac{\pi}{2x}} J_{n+1/2}(x)$ are spherical Bessel functions:

$$\begin{aligned} j_1(x) &= \frac{\sin x}{x^2} - \frac{\cos x}{x} = \frac{1}{3}x - \frac{1}{30}x^3 + \mathcal{O}(x^5), \quad (20) \\ j_2(x) &= \left(\frac{3}{x^2} - 1 \right) \frac{\sin x}{x} - \frac{3 \cos x}{x^2} \\ &= \frac{1}{15}x^2 - \frac{1}{210}x^4 + \mathcal{O}(x^6). \quad (21) \end{aligned}$$

We immediately see that in the limit $kr \rightarrow 0$ only the first term in Eq. (19) survives and d_{ab} reduces to r_{ab} , as it should. Restricting ourselves to the next term of the expansion in kr , we get the correction to the radial integral $d_{ab} - r_{ab} \approx \delta d_{ab}$, where

$$\begin{aligned} \delta d_{ab} &= \int_0^\infty r^3 dr \left\{ -\frac{(kr)^2}{10} \left[g_a(r)g_b(r) + f_a(r)f_b(r) \right] \right. \\ &\quad \left. + \frac{kr}{5} \left[\frac{\kappa_a - \kappa_b + 2}{2} g_a(r)f_b(r) \right. \right. \\ &\quad \left. \left. + \frac{\kappa_a - \kappa_b - 2}{2} f_a(r)g_b(r) \right] \right\}. \quad (22) \end{aligned}$$

TABLE I. Self-energy correction to the decay rate of the $2p_{1/2}$ state, in terms of \mathcal{R}_{se} defined by Eq. (25).

Z	This work	Ref. [28]	$Z\alpha$ -expansion
2	-0.003 55 (4)		-0.00343
3	-0.007 00 (3)		-0.00670
4	-0.011 23 (2)		-0.0106
5	-0.016 13 (3)	-0.014	-0.0151
10	-0.047 62 (5)	-0.045	-0.0409
20	-0.131 25 (2)	-0.126	-0.0860
30	-0.230 11 (2)	-0.230	-0.0917
40	-0.339 52 (2)	-0.334	
50	-0.459 30 (1)	-0.449	
60	-0.591 32 (1)	-0.583	
70	-0.738 41 (1)	-0.738	
80	-0.903 81 (1)	-0.921	
90	-1.090 11 (1)	-1.144	
100	-1.296 02 (1)	-1.426	

For the emission of the photon we need to substitute k with $-k$ in the expressions (19) and (22). This keeps the first term in the integral (22) unchanged, but changes sign of the second one. However, if we simultaneously interchange the initial and final states, $a \leftrightarrow b$, we get the same result: $\delta d_{ab}(k) = \delta d_{ba}(-k)$.

The frequency-dependent corrections are suppressed by the ratio of the size of the atom to the transition wavelength. They are typically very small for most of experimentally studied cases of valence transitions in neutral and slightly ionized atoms, as follows from a simple estimate. For example, the $6s_{1/2} \rightarrow 6p_{1/2}$ transition in neutral Cs has frequency $\omega = 11178 \text{ cm}^{-1}$. Taking into account the values of the rms radii of the $6s_{1/2}$ and $6p_{1/2}$ orbitals of 0.34 nm and 0.46 nm, respectively, the first term in Eq. (22) is estimated to be about $\frac{(kr)^2}{10} r_{ab} \sim 8 \cdot 10^{-7} r_{ab}$. The second term includes products of the upper and lower components, so it is about $\frac{(kr)\alpha}{5} r_{ab} \sim 4 \cdot 10^{-6} r_{ab}$. The frequency-dependent correction for neutral cesium is thus negligibly small even compared to the QED correction.

However, the situation changes drastically for heavy highly ionized ions, because the transition energy grows typically as the square of the effective nuclear charge. Our explicit calculations presented in the next section show that for H-like cesium the frequency-dependent corrections enter already at the percent level.

III. RESULTS AND DISCUSSION

It is convenient to represent numerical results for the self-energy correction to the $E1$ transition amplitude in terms of the multiplicative function $\mathcal{R}_{\text{se}}(Z\alpha)$ defined as

$$\delta z_{\text{se}} = z_{ab} \frac{\alpha}{\pi} \mathcal{R}_{\text{se}}(Z\alpha). \quad (23)$$

We start with comparing our numerical results with the numerical values obtained for the $2p_{1/2}$ - $1s$ transition by

TABLE II. Self-energy corrections to the $E1$ amplitude of the $1s$ - $2p_{1/2}$ transition of H-like ions, in terms of $\mathcal{R}_{\text{se}}(Z\alpha)$ defined by Eq. (23). r_{ab} are the zeroth-order radial integrals defined by Eq. (8) in r.u.

Z	$ r_{ab} $	po	vr, free	vr, many	se
2	88.3999	0.00553	-0.18863	0.18861 (2)	0.00550 (2)
3	58.9278	0.01095	-0.18777	0.18773 (1)	0.01091 (1)
4	44.1901	0.01764	-0.18674	0.18668 (1)	0.01759 (1)
5	35.3462	0.02539	-0.18558	0.18549 (1)	0.02530 (1)
10	17.6485	0.07578	-0.17876	0.17849 (2)	0.07551 (2)
20	8.7747	0.21153	-0.16408	0.16314 (1)	0.21059 (1)
30	5.7940	0.37233	-0.15086	0.14880 (1)	0.37026 (1)
40	4.2855	0.54808	-0.13929	0.13592 (1)	0.54470 (1)
50	3.3647	0.73564	-0.12840	0.12394 (1)	0.73117 (1)
55	3.0241	0.83391	-0.12283	0.11804 (1)	0.82912 (1)
60	2.7364	0.93556	-0.11692	0.11204 (1)	0.93067 (1)
70	2.2735	1.15148	-0.10336	0.09937	1.14749
80	1.9119	1.39117	-0.08601	0.08501	1.39017
90	1.6151	1.66955	-0.06269	0.06787	1.67474
100	1.3600	2.01683	-0.03027	0.04659	2.03315

Sapirstein, Pachucki and Cheng [28] and with the leading terms of the $Z\alpha$ expansion derived in that work. In that work results were obtained in the form of corrections to the $2p_{1/2}$ -state decay rate, rather than amplitudes, so we need to connect the transition amplitude z_{ab} to the decay rate Γ_{ab} . This is achieved by observing that

$$\frac{\delta\Gamma_{ab}}{\Gamma_{ab}} = 3 \frac{\delta E_{ab}}{E_{ab}} + 2 \frac{\delta z_{ab}}{z_{ab}}, \quad (24)$$

where E_{ab} and δE_{ab} is the zero-order energy difference between the states a and b and its correction, respectively. The self-energy correction to Γ_{ab} can then be represented in a form analogous to Eq. (23),

$$\delta\Gamma_{\text{se}} = \Gamma_{ab} \frac{\alpha}{\pi} \mathcal{R}_{\text{se}}(Z\alpha). \quad (25)$$

To the leading order in $Z\alpha$, the self-energy correction to the $2p_{1/2}$ decay rate is [28, 29]

$$\mathcal{R}_{\text{se}}(Z\alpha) = (Z\alpha)^2 \left\{ \left[\frac{8}{3} \ln \frac{4}{3} - \frac{61}{18} \right] \ln(Z\alpha)^{-2} + 6.05168 \right\}. \quad (26)$$

Results of our numerical calculations of the self-energy correction to the decay rate of the $2p_{1/2}$ state are presented in Table I, in comparison with predictions of the $Z\alpha$ expansion and all-order numerical results obtained in Ref. [28]. We observe that both numerical calculations converge to the $Z\alpha$ -expansion predictions in the low- Z limit but significantly deviate from them for medium- and high- Z values. The two numerical calculations are in reasonable agreement with each other. We observe small deviations increasing with the increase of Z , probably due to different nuclear models used in the calculations. (Ref. [28] used a finite-size nucleus, whereas we use the point nuclear model.) Small deviations observed for the lowest Z are probably due to numerical issues. It

TABLE III. Self-energy corrections to the $ns-n'p$ $E1$ matrix elements for H-like Cs ($Z = 55$) in terms of $R_{se}(Z\alpha)$ defined by Eq. (23). r_{ab} and δd_{ab} are the zeroth-order radial integrals and frequency-dependent corrections defined by Eqs. (8) and (22) respectively, in r.u.; “qmod” labels approximate results obtained with the QEDMOD package.

a	b	$ r_{ab} $	$10^3 \frac{\delta d_{ab}(\omega)}{r_{ab}}$	po	vr	se	qmod	$\frac{\text{qmod-po}}{\text{po}}, \%$	$\frac{\text{qmod-se}}{\text{se}}, \%$
1s	2p _{1/2}	3.0241	11.73	0.83391	-0.00480	0.82910 (1)	0.866	3.8	4.4
1s	3p _{1/2}	1.1647	20.73	0.54248	-0.04076 (6)	0.50172 (6)	0.560	3.2	11.6
1s	4p _{1/2}	0.6760	23.86	0.46690	-0.0573 (3)	0.4096 (3)	0.480	2.8	17.1
1s	5p _{1/2}	0.4595	25.29	0.43673 (5)	-0.0661 (4)	0.3706 (4)	0.446	2.2	20.4
1s	6p _{1/2}	0.3450	26.07	0.4219 (5)	-0.072 (2)	0.350 (2)	0.429	1.7	22.5
1s	2p _{3/2}	3.0161	-36.04	0.81139	0.03740 (1)	0.84879 (1)	0.838	3.3	-1.2
1s	3p _{3/2}	1.2341	-36.05	0.59164	0.0089 (1)	0.6006 (1)	0.578	-2.4	-3.8
1s	4p _{3/2}	0.7304	-36.03	0.53484 (1)	-0.0044 (5)	0.5304 (5)	0.500	-6.6	-5.8
1s	5p _{3/2}	0.5010	-36.03	0.51263 (5)	-0.0118 (5)	0.5008 (5)	0.466	-9.1	-7.0
1s	6p _{3/2}	0.3787	-36.03	0.5020 (6)	-0.016 (1)	0.486 (1)	0.449	-10.6	-7.7
2s	2p _{1/2}	12.0497	0.00	0.02819	0.02164	0.04983	0.054	92.7	9.0
2s	3p _{1/2}	7.3677	-0.01	1.05192	0.01590 (1)	1.06782 (2)	1.078	2.5	1.0
2s	4p _{1/2}	3.0501	2.98	0.66348	0.0061 (1)	0.6696 (1)	0.686	3.3	2.4
2s	5p _{1/2}	1.8309	4.35	0.54219 (5)	-0.001 (2)	0.541 (2)	0.558	3.0	3.3
2s	6p _{1/2}	1.2931	5.09	0.4861 (5)	-0.007 (2)	0.479 (2)	0.499	2.6	4.0
2s	2p _{3/2}	12.5733	-0.38	0.07397	0.02306 (1)	0.09703 (1)	0.100	35.0	2.9
2s	3p _{3/2}	6.6065	-9.61	1.07766	0.0255 (1)	1.1031 (1)	1.100	2.0	-0.3
2s	4p _{3/2}	2.8941	-9.80	0.73978 (1)	0.0177 (1)	0.7575 (1)	0.752	1.6	-0.8
2s	5p _{3/2}	1.7713	-9.88	0.63274 (5)	0.012 (3)	0.644 (3)	0.637	0.7	-1.1
2s	6p _{3/2}	1.2646	-9.92	0.5838 (6)	0.008 (2)	0.591 (2)	0.583	-0.1	-1.4
3s	2p _{1/2}	2.2735	-11.71	-1.89331 (5)	0.05923 (7)	-1.83408 (8)	-1.855	-2.0	1.1
3s	3p _{1/2}	30.1688	0.00	0.02006	0.01108 (4)	0.03114 (4)	0.030	47.3	-5.1
3s	4p _{1/2}	13.2394	-0.81	1.16592 (3)	0.0119 (2)	1.1778 (2)	1.185	1.6	0.6
3s	5p _{1/2}	5.4498	0.55	0.75111 (5)	0.009 (2)	0.760 (2)	0.768	2.2	1.0
3s	6p _{1/2}	3.3201	1.29	0.6120 (5)	0.006 (1)	0.618 (2)	0.625	2.2	1.2
3s	2p _{3/2}	2.9421	-1.35	-1.41360 (4)	0.04475 (5)	-1.36884 (7)	-1.372	-3.0	0.2
3s	3p _{3/2}	30.9663	-0.11	0.06368	0.0114 (1)	0.0750 (1)	0.075	18.5	0.6
3s	4p _{3/2}	11.5084	-4.31	1.21398 (3)	0.0162 (2)	1.2302 (2)	1.224	0.9	-0.5
3s	5p _{3/2}	5.0114	-4.44	0.83882 (5)	0.015 (3)	0.854 (3)	0.846	0.9	-0.9
3s	6p _{3/2}	3.1179	-4.50	0.7107 (6)	0.013 (2)	0.723 (2)	0.715	0.5	-1.2
4s	2p _{1/2}	0.9285	-12.73	-1.61639 (1)	0.0777 (3)	-1.5387 (3)	-1.565	-3.2	1.7
4s	3p _{1/2}	5.8984	-4.90	-1.75260 (2)	0.0260 (4)	-1.7266 (4)	-1.726	-1.5	0.0
4s	4p _{1/2}	55.7204	0.00	0.01608	0.00658 (4)	0.02266 (4)	0.020	25.9	-10.7
4s	5p _{1/2}	20.7063	-0.74	1.23126 (3)	0.008 (3)	1.239 (3)	1.244	1.0	0.4
4s	6p _{1/2}	8.4931	-0.01	0.8089 (4)	0.0076 (9)	0.817 (1)	0.822	1.6	0.6
4s	2p _{3/2}	1.1473	1.01	-1.15431 (1)	0.0581 (3)	-1.0962 (3)	-1.100	-4.7	0.3
4s	3p _{3/2}	7.4789	-1.15	-1.33755 (2)	0.0204 (4)	-1.3172 (4)	-1.310	-2.0	-0.5
4s	4p _{3/2}	56.7637	-0.05	0.05716	0.00668 (9)	0.06384 (9)	0.064	11.3	-0.3
4s	5p _{3/2}	17.7224	-2.44	1.29323 (4)	0.011 (2)	1.304 (2)	1.291	-0.2	-1.0
4s	6p _{3/2}	7.6985	-2.52	0.9047 (5)	0.011 (1)	0.916 (1)	0.905	0.0	-1.2
5s	2p _{1/2}	0.5542	-13.20	-1.53456 (5)	0.083 (2)	-1.451 (2)	-1.481	-3.5	2.1
5s	3p _{1/2}	2.3455	-5.41	-1.44462 (4)	0.037 (4)	-1.408 (4)	-1.407	-2.6	0.0
5s	4p _{1/2}	11.1399	-2.63	-1.67961 (4)	0.014 (6)	-1.665 (6)	-1.665	-0.8	0.0
5s	5p _{1/2}	88.7317	0.00	0.01350 (1)	0.00 (2)	0.02 (2)	0.016	15.2	-9.7
5s	6p _{1/2}	30.0484	-0.60	1.2729 (3)	0.007 (4)	1.280 (4)	1.282	0.7	0.2
5s	2p _{3/2}	0.6751	2.10	-1.07852 (5)	0.062 (2)	-1.017 (2)	-1.022	-5.2	0.5
5s	3p _{3/2}	2.8397	-0.08	-1.04889 (3)	0.028 (3)	-1.021 (3)	-1.013	-3.4	-0.7
5s	4p _{3/2}	13.9450	-0.84	-1.29713 (4)	0.012 (3)	-1.285 (3)	-1.271	-2.0	-1.1
5s	5p _{3/2}	90.0012	-0.03	0.05275 (1)	0.005 (4)	0.058 (4)	0.057	7.5	-2.5
5s	6p _{3/2}	25.5038	-1.56	1.3443 (3)	0.010 (6)	1.354 (6)	1.333	-0.8	-1.5
6s	2p _{1/2}	0.3902	-13.44	-1.4959 (7)	0.085 (2)	-1.411 (2)	-1.443	-3.6	2.3
6s	3p _{1/2}	1.4054	-5.68	-1.3534 (6)	0.041 (2)	-1.313 (2)	-1.312	-3.0	0.0
6s	4p _{1/2}	4.3917	-2.91	-1.3525 (5)	0.020 (2)	-1.332 (2)	-1.331	-1.6	-0.1
6s	5p _{1/2}	18.1437	-1.62	-1.6352 (3)	0.011 (6)	-1.624 (6)	-1.627	-0.5	0.2
6s	6p _{1/2}	127.2007	0.00	0.0117 (3)	0.003 (3)	0.015 (3)	0.013	8.8	-15.1
6s	2p _{3/2}	0.4723	2.69	-1.0426 (7)	0.0620 (7)	-0.981 (1)	-0.987	-5.4	0.6
6s	3p _{3/2}	1.6771	0.50	-0.9647 (6)	0.030 (2)	-0.934 (2)	-0.926	-4.0	-0.9
6s	4p _{3/2}	5.2457	-0.25	-0.9907 (5)	0.016 (1)	-0.975 (2)	-0.961	-3.0	-1.5
6s	5p _{3/2}	22.5169	-0.62	-1.2720 (2)	0.009 (3)	-1.263 (3)	-1.245	-2.1	-1.4
6s	6p _{3/2}	128.6106	-0.01	0.0496 (3)	0.004 (5)	0.054 (5)	0.052	5.2	-2.8

TABLE IV. Self-energy corrections to $np-n'd$ $E1$ matrix elements in H-like Cs. Notations and units are as in Table III.

a	b	$ r_{ab} $	$10^3 \frac{\delta d_{ab}(\omega)}{r_{ab}}$	po	vr	se	qmod	$\frac{\text{qmod-po}}{\text{po}}, \%$	$\frac{\text{qmod-se}}{\text{se}}, \%$
$2p_{1/2}$	$3d_{3/2}$	10.8136	-3.28	0.01139	0.00526 (3)	0.01665 (3)	0.024	108.6	42.7
$2p_{1/2}$	$4d_{3/2}$	4.0780	-1.60	0.00961 (1)	-0.0105 (3)	-0.0009 (3)	0.009	-9.2	-1075.9
$2p_{1/2}$	$5d_{3/2}$	2.3589	-0.82	0.01274 (2)	-0.0199 (1)	-0.0071 (1)	0.002	-86.7	-123.8
$2p_{3/2}$	$3d_{3/2}$	11.5701	5.53	0.05593	-0.00154 (7)	0.05439 (7)	0.069	24.2	27.8
$2p_{3/2}$	$4d_{3/2}$	4.0892	10.41	0.00906 (1)	-0.0211 (3)	-0.0120 (3)	0.007	-24.4	-157.0
$2p_{3/2}$	$5d_{3/2}$	2.3118	12.68	-0.00309 (2)	-0.03228 (4)	-0.03536 (5)	-0.017	454.9	-51.5
$3p_{1/2}$	$3d_{3/2}$	24.7424	-0.03	-0.01610	0.01015 (8)	-0.00595 (8)	-0.009	-41.2	59.1
$3p_{1/2}$	$4d_{3/2}$	16.6721	-2.06	0.03348	0.0081 (1)	0.0416 (1)	0.048	42.1	14.4
$3p_{1/2}$	$5d_{3/2}$	6.9098	-1.28	0.01781 (2)	0.0016 (2)	0.0194 (2)	0.024	32.8	21.8
$3p_{3/2}$	$3d_{3/2}$	24.5288	0.00	-0.02471	0.01077 (5)	-0.01393 (5)	-0.017	-31.1	22.2
$3p_{3/2}$	$4d_{3/2}$	18.6295	1.17	0.09649 (1)	0.0052 (1)	0.1017 (1)	0.113	17.4	11.5
$3p_{3/2}$	$5d_{3/2}$	7.2515	3.41	0.04023 (2)	-0.0027 (2)	0.0375 (2)	0.048	19.7	28.4
$4p_{1/2}$	$3d_{3/2}$	4.1851	-2.81	-0.12454 (1)	0.0258 (4)	-0.0988 (4)	-0.095	-24.1	-4.2
$4p_{1/2}$	$4d_{3/2}$	51.1988	-0.01	-0.00999	0.00610 (2)	-0.00389 (2)	-0.007	-28.4	83.8
$4p_{1/2}$	$5d_{3/2}$	23.8664	-1.39	0.04863 (2)	0.0068 (2)	0.0555 (2)	0.060	23.6	8.4
$4p_{3/2}$	$3d_{3/2}$	3.2484	-6.70	-0.32191 (3)	0.0337 (5)	-0.2882 (5)	-0.302	-6.1	4.9
$4p_{3/2}$	$4d_{3/2}$	50.9107	0.00	-0.01661	0.00641 (6)	-0.01020 (6)	-0.013	-20.0	30.2
$4p_{3/2}$	$5d_{3/2}$	27.2582	0.18	0.11999 (2)	0.00508 (3)	0.12507 (4)	0.140	16.5	11.8
$5p_{1/2}$	$3d_{3/2}$	1.4993	-2.54	-0.12417 (3)	0.0394 (5)	-0.0848 (5)	-0.079	-36.5	-7.0
$5p_{1/2}$	$4d_{3/2}$	9.5709	-1.62	-0.10980 (4)	0.01393 (9)	-0.0959 (1)	-0.097	-11.7	1.1
$5p_{1/2}$	$5d_{3/2}$	84.7700	-0.01	-0.00673 (1)	0.00408 (5)	-0.00265 (5)	-0.005	-20.8	101.5
$5p_{3/2}$	$3d_{3/2}$	1.2081	-8.09	-0.30312 (4)	0.051 (1)	-0.252 (1)	-0.272	-10.3	7.9
$5p_{3/2}$	$4d_{3/2}$	7.5474	-3.48	-0.28786 (7)	0.0177 (2)	-0.2702 (2)	-0.297	3.3	10.1
$5p_{3/2}$	$5d_{3/2}$	84.4356	0.00	-0.01228 (1)	0.0042 (2)	-0.0081 (2)	-0.011	-11.4	34.8

should be mentioned that Ref. [28] used a completely different approach to the calculation of the decay rates, via the imaginary part of the two-loop self-energy. The observed agreement of the two calculations is also a check of consistency of the two different approaches.

Table II presents results of our numerical calculations of the self-energy correction to the $E1$ matrix elements of the $1s-2p_{1/2}$ transition along the hydrogen isoelectronic sequence. We observe large cancellations between the free-electron and many-potential parts of the vr correction, thus corroborating the findings of Ref. [28], which reported large numerical cancellations at intermediate stages of calculations. These cancellations are particularly pronounced in the low- Z region. For instance, at $Z = 2$, the first four digits cancel out. This highlights the need for meticulous control of numerical accuracy throughout the intermediate stages of these calculations. We also observe that the vr contribution is much smaller than the po correction in the whole region of nuclear charges, accounting for typically about 1% of the total self-energy correction.

We now turn to the detailed analysis of the $E1$ transition matrix elements between different states of a selected H-like ion. We have chosen the reference ion to be cesium ($Z = 55$), since it is well studied experimentally (see, e. g. Refs. [30–33]) and its nuclear charge is large enough for QED effects to be of experimental interest. Table III presents our numerical results for the $ns-n'p$ matrix elements, whereas Table IV summarizes our results obtained for the $np-n'd$ transitions.

Tables III and IV include values for the relative frequency-

dependent correction $\frac{\delta d_{ab}(\omega)}{r_{ab}}$, multiplied by 10^3 . They are calculated using Eq. (22) and taking the transition energy as the difference of the Dirac energies of the initial and the final state. We observe that the frequency-dependent correction is typically at a percent (sometimes, a few percent) level and thus should be taken into account for H-like ions. By contrast, it becomes negligibly small for neutral and slightly ionized ions. For example, if we recalculate this correction with the same hydrogenic wave functions but with frequency $\omega = 11178 \text{ cm}^{-1}$ corresponding the $6s_{1/2} \rightarrow 6p_{1/2}$ transition in neutral Cs, we obtain the relative contribution on the 10^{-6} level, which is much smaller than the QED corrections.

Table III and IV presents our numerical results for the self-energy correction for the $ns-n'p$ and $np-n'd$ transitions. We observe that the dependence of the self-energy corrections of the (n, n') matrix elements on n and n' turns out to be rather complicated. In particular, for the (n, n) matrix elements the self-energy corrections are abnormally suppressed, even after taking into account that the zeroth-order radial integrals r_{ab} reach their maximal values in this case. Furthermore, for $n < n'$ and $n > n'$ the corrections are typically of the opposite sign. We conclude that the self-energy correction to the $E1$ matrix elements does not have a well-defined sign and can both increase and decrease the absolute values of the transition amplitude.

In the last three columns of Tables III and IV we compare our ab initio values with approximate self-energy results obtained with help of QEDMOD package (with the vacuum-

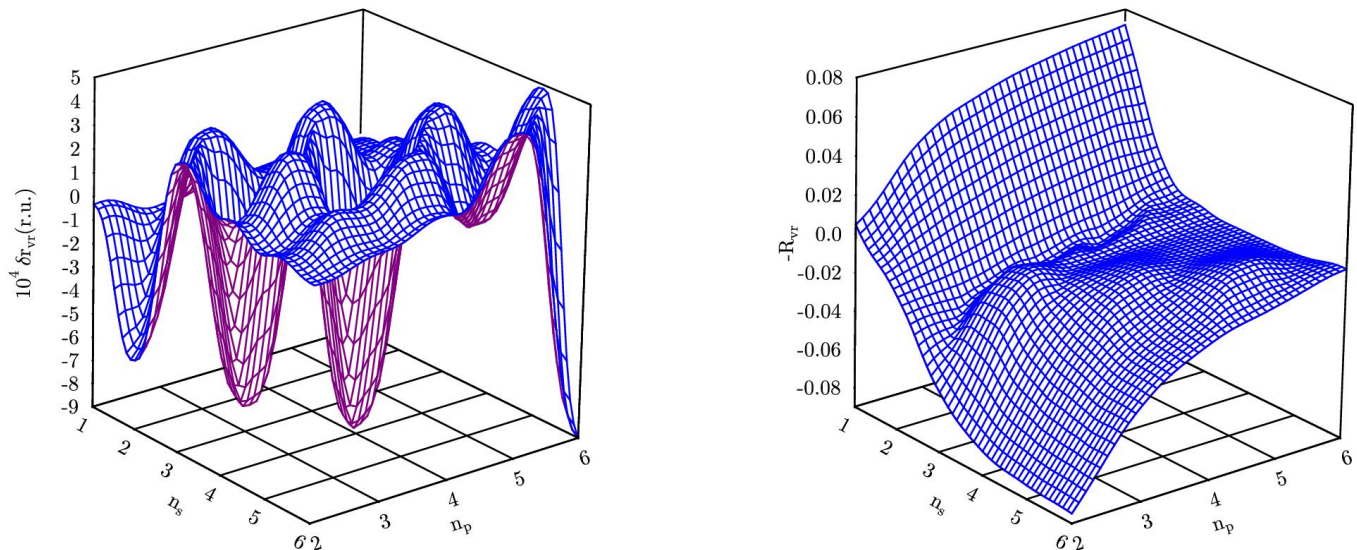


FIG. 1. Vertex-reducible (vr) QED correction to the $n_s s_{1/2} \rightarrow n_p p_{1/2}$ transitions in H-like Cs ion. Left panel: corrections to the radial integrals r_{ab} ; right panel: corrections to the scaled function R_{se} defined by Eq. (23), multiplied by (-1) for better vision.

polarization part switched off). We recall that the QEDMOD results should approximately reproduce the po part of the ab initio se correction, whereas the vr part is omitted in the approximate treatment.

We see that for the $ns-n'p$ matrix elements QEDMOD calculations reproduce the po values very well in most cases. The exception is the diagonal (n, n) matrix elements, where the deviation may reach 90% (for the $(2s, 2p_{1/2})$ transition). In this case the po contribution is abnormally small, and the absolute error turns out to be not very significant. The vr part of the se correction is also relatively small for the $ns-n'p$ matrix elements. As a result, we may conclude that the QEDMOD treatment, despite ignoring the vr contribution, still reproduces the ab initio se correction reasonably well, the typical accuracy being within 10% in most cases.

For the $np-n'd$ matrix elements, however, the situation is different. First, the po part is significantly smaller in magnitude than for the $ns-n'p$ matrix elements, leading to significantly smaller se corrections. Next, the po and vr parts are of the same order. Furthermore, the QEDMOD calculations do not reproduce well even the po part of the se correction. We conclude that for the $np-n'd$ matrix elements, the QEDMOD treatment provides only the order of magnitude of the se contribution, but is not capable of yielding a quantitative approximation.

It is important to note that the situation in many-electron atoms can differ significantly from that of hydrogen-like ions. In particular, many-electron atoms often exhibit substantial mixing of single-electron configurations due to electron correlation effects. For the $p-d$ transitions, where QED effects on radial integrals are relatively small, a more significant QED contribution may arise from the configuration mixing. For example, this was the case in our recent study of the ten-electron ions Fe^{16+} and Ni^{18+} [17], where the dominant QED correc-

tion to the $2p-3d$ transitions was found to originate from electronic correlations. It was demonstrated that such corrections can be effectively accounted for by incorporating the QEDMOD potential in many-electron calculations.

The matrix elements of the QED corrections to the transition amplitudes in the hydrogenic basis, obtained in this work, could, in principle, be used to construct a model operator analogous to QEDMOD but specifically tailored for the $E1$ transition amplitude. As noted earlier, the po part of these QED corrections can be sufficiently accurately accounted for by using the QEDMOD potential. Therefore, an additional model operator would only need to account for the vr correction. To evaluate the feasibility of such a project, Fig. 1 presents the vr correction for the $n_s s_{1/2} \rightarrow n_p p_{1/2}$ transitions in hydrogen-like cesium as a function of the quantum numbers n_s and n_p . The left panel displays the vr correction to the radial integrals r_{ab} , while the right panel shows these corrections to the scaled function R_{se} . The corrections to the radial integrals exhibit highly complex and irregular behavior. The dependence of the scaled function is more regular but nevertheless remains quite complex. Notably, the sign of the correction differs between cases where $n_s < n_p$ and $n_s > n_p$. This complex behavior might indicate that the vr correction originates not only from small distances, as is typical for QED effects, but also from large distances. The intricate dependence of the vr correction on the principal quantum numbers of the transition states significantly complicates the construction of an effective operator.

IV. SUMMARY

We performed ab initio calculations of the self-energy correction to the $E1$ transition amplitudes in H-like ions, to all

orders in the binding nuclear strength parameter $Z\alpha$. Our results for the $1s-2p_{1/2}$ transition amplitude were converted to the correction to the decay rate of the $2p_{1/2}$ state and compared with previous all-order and $Z\alpha$ -expansion calculations [28]. Good agreement was found, which yields an important check of consistency of different methods. Our calculation confirms the previous conclusion of Ref. [16] that the vertex and reducible parts of the self-energy correction are small, their contribution being on the level of 1% for the $1s-2p_{1/2}$ matrix element.

A detailed study of self-energy correction for a large number of $ns-n'p$ and $np-n'd$ transitions was carried out for H-like cesium. We found a complicated dependence of the self-energy corrections of the (n, n') matrix elements on n and n' . We conclude that for the $ns-n'p$ matrix elements, the perturbed-orbital contribution is dominant and the vertex and reducible corrections are relatively small, so that the total self-

energy effect can usually be well reproduced by approximate calculations with the QEDMOD model potential. By contrast, for the $np-n'd$ matrix elements we find significantly smaller self-energy corrections, which are not well reproduced by the QEDMOD model potential.

The comparison of our ab initio results with approximate treatment based on the QEDMOD model potential allows one to estimate uncertainties associated with usage of the QEDMOD potential in many-electron calculations of the $E1$ transition amplitudes in multi-electron atoms [2, 3, 9–11].

ACKNOWLEDGMENTS

We are grateful to Andrey Bondarev and to Ilya Tupitsyn for the help with calculations of the frequency-dependent corrections to the radial integrals. This work was supported by the Russian Science Foundation grant #23-22-00079.

-
- [1] S. Kühn, C. Shah, J. R. C. López-Urrutia, K. Fujii, R. Steinbrügge, J. Stierhof, M. Togawa, Z. Harman, N. S. Oreshkina, C. Cheung, M. G. Kozlov, S. G. Porsev, M. S. Safronova, J. C. Berengut, M. Rosner, M. Bissinger, R. Ballhausen, N. Hell, S. Park, M. Chung, M. Hoesch, J. Seltmann, A. S. Surzhykov, V. A. Yerokhin, J. Wilms, F. S. Porter, T. Stöhlker, C. H. Keitel, T. Pfeifer, G. V. Brown, M. A. Leutenegger, and S. Bernitt, High resolution photoexcitation measurements exacerbate the long-standing Fe XVII oscillator strength problem, *Phys. Rev. Lett.* **124**, 225001 (2020), arXiv:1911.09707.
- [2] S. Kühn, C. Cheung, N. S. Oreshkina, R. Steinbrügge, M. Togawa, S. Bernitt, L. Berger, J. Buck, M. Hoesch, J. Seltmann, F. Trinter, C. H. Keitel, M. G. Kozlov, S. G. Porsev, M. F. Gu, F. S. Porter, T. Pfeifer, M. A. Leutenegger, Z. Harman, M. S. Safronova, J. R. C. López-Urrutia, and C. Shah, New Measurement Resolves Key Astrophysical Fe XVII Oscillator Strength Problem, *Phys. Rev. Lett.* **129**, 245001 (2022), arXiv:2201.09070.
- [3] C. Shah, S. Kühn, S. Bernitt, R. Steinbrügge, M. Togawa, L. Berger, J. Buck, M. Hoesch, J. Seltmann, M. G. Kozlov, S. G. Porsev, M. F. Gu, F. Scott Porter, T. Pfeifer, M. A. Leutenegger, C. Cheung, M. S. Safronova, and J. R. C. López-Urrutia, Natural-linewidth measurements of the 3C and 3D soft-x-ray transitions in Ni XIX, *Phys. Rev. A* **109**, 063108 (2024).
- [4] M. S. Safronova, D. Budker, D. DeMille, D. F. Jackson Kimball, A. Derevianko, and C. W. Clark, Search for New Physics with Atoms and Molecules, *Rev. Mod. Phys.* **90**, 025008 (2018), arXiv:1710.01833.
- [5] V. M. Shabaev, I. I. Tupitsyn, K. Pachucki, G. Plunien, and V. A. Yerokhin, Radiative and correlation effects on the parity-nonconserving transition amplitude in heavy alkali-metal atoms, *Phys. Rev. A* **72**, 062105 (2005).
- [6] C. S. Wood, S. C. Bennett, D. Cho, B. P. Masterson, J. L. Roberts, C. E. Tanner, and C. E. Wieman, Measurement of parity nonconservation and an anapole moment in cesium, *Science* **275**, 1759 (1997).
- [7] J. Sapirstein and K. T. Cheng, Calculation of the Lamb shift in neutral alkali metals, *Phys. Rev. A* **66**, 042501 (2002).
- [8] J. Sapirstein and K. T. Cheng, Calculation of radiative corrections to hyperfine splittings in the neutral alkali metals, *Phys. Rev. A* **67**, 022512 (2003).
- [9] C. J. Fairhall, B. M. Roberts, and J. S. M. Ginges, QED radiative corrections to electric dipole amplitudes in heavy atoms, *Phys. Rev. A* **107**, 022813 (2023), arXiv:2212.11490.
- [10] B. M. Roberts, C. J. Fairhall, and J. S. M. Ginges, Electric-dipole transition amplitudes for atoms and ions with one valence electron, *Phys. Rev. A* **107**, 052812 (2023), arXiv:2211.11134.
- [11] H. B. Tran Tan and A. Derevianko, Precision theoretical determination of electric-dipole matrix elements in atomic cesium, *Phys. Rev. A* **107**, 042809 (2023).
- [12] M. G. Kozlov, Y. A. Demidov, M. Y. Kaygorodov, and E. V. Tryapitsyna, Basis set calculations of heavy atoms, *Atoms* **12**, 3 (2024), arXiv:2312.07782.
- [13] V. M. Shabaev, I. I. Tupitsyn, and V. A. Yerokhin, Model operator approach to the Lamb shift calculations in relativistic many-electron atoms, *Phys. Rev. A* **88**, 012513 (2013).
- [14] V. M. Shabaev, I. I. Tupitsyn, and V. A. Yerokhin, QEDMOD: Fortran program for calculating the model Lamb-shift operator, *Comp. Phys. Comm.* **189**, 175 (2015).
- [15] V. M. Shabaev, I. I. Tupitsyn, and V. A. Yerokhin, QEDMOD: Fortran program for calculating the model Lamb-shift operator, *Comp. Phys. Comm.* **223**, 69 (2018).
- [16] J. Sapirstein and K. T. Cheng, Calculation of radiative corrections to $E1$ matrix elements in the neutral alkali metals, *Phys. Rev. A* **71**, 022503 (2005).
- [17] M. G. Kozlov, V. A. Yerokhin, M. Y. Kaygorodov, and E. V. Tryapitsyna, QED calculations of the $E1$ transition amplitude in neonlike iron and nickel, *Phys. Rev. A* **110**, 062805 (2024), arXiv:2410.02489.
- [18] V. M. Shabaev, Two-time Green's function method in quantum electrodynamics of high- Z few-electron atoms, *Phys. Rep.* **356**, 119 (2002).
- [19] V. Yerokhin and V. Shabaev, First-order self-energy correction in hydrogenlike systems, *Phys. Rev. A* **60**, 800 (1999).
- [20] V. A. Yerokhin and A. V. Maiorova, Calculations of QED Effects with the Dirac Green Function, *Symmetry* **12**, 800 (2020).
- [21] D. Varshalovich, A. Moskalev, and V. Khersonskii, *Quantum theory of angular momentum* (World Scientific, 1988).

- [22] V. Yerokhin, A. Artemyev, T. Beier, G. Plunien, V. Shabaev, and G. Soff, Two-electron self-energy corrections to the $2p\ 1/2-2s$ transition energy in Li-like ions, *Phys. Rev. A* **60**, 3522 (1999).
- [23] H. Persson, S. Salomonson, P. Sunnergren, and I. Lindgren, Radiative corrections to the electron g-factor in H-like ions, *Phys. Rev. A* **56**, R2499 (1997).
- [24] V. A. Yerokhin and V. M. Shabaev, First order self-energy correction in hydrogen-like systems, *Phys. Rev. A* **60**, 800 (1999).
- [25] I. P. Grant, Gauge invariance and relativistic radiative transitions, *J. Phys. B: Atomic and Molecular Physics* **7**, 1458 (1974).
- [26] W. R. Johnson, *Atomic Structure Theory. Lectures on Atomic Physics* (Springer Berlin Heidelberg, 2007).
- [27] R. V. Popov and A. V. Maiorova, Relativistic calculations of one-photon transition probabilities in hydrogen-like ions, *Optics and Spectroscopy* **122**, 366 (2017).
- [28] J. Sapirstein, K. Pachucki, and K. T. Cheng, Radiative corrections to one-photon decays of hydrogenic ions, *Phys. Rev. A* **69**, 022113 (2004), arXiv:hep-ph/0311134.
- [29] V. G. Ivanov and S. G. Karshenboim, Radiative corrections to dipole matrix elements in hydrogen-like atoms, *Phys. Lett. A* **210**, 313 (1996).
- [30] G. Toh, A. Damitz, N. Glotzbach, J. Quirk, I. C. Stevenson, J. Choi, M. S. Safronova, and D. S. Elliott, Electric dipole matrix elements for the $6p^2P_J \rightarrow 7s^2S_{1/2}$ transition in atomic cesium, *Phys. Rev. A* **99**, 032504 (2019).
- [31] G. Toh, N. Chalus, A. Burgess, A. Damitz, P. Imany, D. E. Leaird, A. M. Weiner, C. E. Tanner, and D. S. Elliott, Measurement of the lifetimes of the $7p^2P_{3/2}$ and $7p^2P_{1/2}$ states of atomic cesium, *Phys. Rev. A* **100**, 052507 (2019).
- [32] G. Toh, A. Damitz, C. E. Tanner, W. R. Johnson, and D. S. Elliott, Determination of the Scalar and Vector Polarizabilities of the Cesium $6s^2S_{1/2} \rightarrow 7s^2S_{1/2}$ Transition and Implications for Atomic Parity Nonconservation, *Phys. Rev. Lett.* **123**, 073002 (2019).
- [33] J. A. Quirk, A. Jacobsen, A. Damitz, C. E. Tanner, and D. S. Elliott, Measurement of the Static Stark Shift of the $7s^2S_{1/2}$ Level in Atomic Cesium, *Phys. Rev. Lett.* **132**, 233201 (2024).